Automatic detection of detached and erroneous electrodes in electrical impedance tomography

Yednek Asfaw, Andy Adler
School of Information Technology and Engineering
University of Ottawa, Ottawa, Canada
yasfaw@site.uottawa.ca, adler@site.uottawa.ca

Short Title: Detection of erroneous electrodes

Keywords: Electrical Impedance Tomography, Image Reconstruction, Data Errors, Electrodes

Corresponding Author: Andy Adler
School of Information Technology and Engineering (SITE),
University of Ottawa
800 King Edward Ave.
Ottawa, Ontario, Canada, K1N 6N5
Tel: (613) 562-5800 ext. 6218, Fax: (613) 562-5664
Email: adler@site.uottawa.ca

Abstract

One unfortunate occurrence in experimental measurements with electrical impedance tomography is electrodes which become detached or poorly connected, such that the measured data cannot be used. This paper presents an automatic approach to detect such erroneous electrodes. It is based on the assumption that all valid measurements are related by the image reconstruction model, while the measurements from erroneous electrodes are unrelated. The method estimates the data at an electrode based on the measurements from all other electrodes, and compares it to the measurements. If these data match adequately, the set of electrodes does not contain an erroneous electrode. In order to detect an erroneous electrode amongst *N* electrodes, all sets of *N-1* electrodes are tested, and the set with the best match between measurements and estimate is identified as the one which excludes the erroneous electrode. The method was tested on simulated and experimental data and showed consistent identification of erroneous electrodes with those made by experts.

Introduction

Electrical Impedance Tomography (EIT) uses body surface electrodes to make measurements from which an image of the conductivity distribution is calculated. However, one important difficulty with experimental and clinical EIT measurements is the care required to ensure accurate current injection and voltage measurement. Many conditions can cause EIT measurements to differ from their correct values, such as interference from electronics (Al-Hatib, 1998, Meeson *et al*, 1996), and poor electrode contact due to patient movement (Blott *et al*, 1998), or sweat and peripheral oedema. This effect is especially important in long term monitoring applications (Lozano *et al*, 1995).

Given a set of data containing measurements with errors, it is desired to calculate an image based on the remaining good data. In order to accomplish this, we have developed a methodology to reconstruct EIT images in the presence of single electrode errors (Adler, 2004). One limitation of that work is the requirement that the erroneous electrodes be identified to the algorithm by an operator. However, the ability to automatically identify erroneous electrodes is a potentially important capability for clinical and experimental applications of EIT. In this paper, we present a method to allow such automatic detection of erroneous electrodes.

Methods

Various heuristic techniques have been used to detect the presence of erroneous electrode data. For example, a test for the presence of faulty electrodes could be based on analysis of images for artefacts, or a test of the measured voltages for unusually large changes. The disadvantage of such heuristic approaches is the difficulty in defining an image artefact, in relation to an unusual, but accurate, measurement. Specifically, it is difficult to define a threshold for changes that could be applied across different systems and injection patterns.

In order to more systematically detect such erroneous electrodes, we propose a method based on comparing the measurements obtained on all electrodes to each other. Since all electrodes measure the same medium, it is reasonable to expect that "good" electrodes will produce measurements consistent with each other. The consistency of a set of electrodes can be verified by estimating the measured data at each electrode in the set, and then comparing the estimate to the actual data measured. A set of electrodes with consistent measurements must contain all "good" electrodes. In order to test an *N* electrode EIT system, we test all possible sets of *N-1* electrodes; if only one of the subsets contains all "good" electrodes, then the electrode excluded from that set must be erroneous.

Image reconstruction with missing data

We consider EIT difference imaging based on the formulation of Adler and Guardo (1996). The forward model estimates the vector of the change in conductivity distribution (**x**) from a vector of change in difference measurements (**z**) and with additive noise (**n**). For small changes in **x**, the relationship is linearized as:

$$\mathbf{z} = \mathbf{Hx} + \mathbf{n} \tag{1}$$

Based on these parameters, the SNR of a measurement is $20\log\|\mathbf{z}\|/\|\mathbf{n}\|$. The Jacobian (sensitivity) matrix (**H**) relates the change in conductivity to change in difference measurements:

$$\mathbf{H}_{i,j} = \left.\frac{\partial \mathbf{z}_i}{\partial \mathbf{x}_j}\right|_{\sigma_b = \sigma_0} \tag{2}$$

The change in conductivity is expressed as the difference in the finite element log conductivities $\mathbf{x} = \log(\sigma^1) - \log(\sigma^2)$, and the normalized difference measurement is defined for the time interval (t^1, t^2) as

$$\mathbf{z} = \frac{\mathbf{v}_i^1 - \mathbf{v}_i^2}{\frac{1}{2}\left(\mathbf{v}_i^1 + \mathbf{v}_i^2\right)} \tag{3}$$

where $\mathbf{v}_i^1$ and $\mathbf{v}_i^2$ represent the ith voltage measurements at time t^1 and t^2, respectively.

The EIT image reconstruction algorithm estimates the change in conductivity ($\hat{\mathbf{x}}$) from measurements **z** using a MAP regularization framework. $\hat{\mathbf{x}}$ is estimated by maximizing the a posteriori probability distribution $f(\mathbf{x}|\mathbf{z})=f(\mathbf{z}|\mathbf{x})f(\mathbf{x})/f(\mathbf{z})$, which simplifies to:

$$\hat{\mathbf{x}} = \left[(\mathbf{H}^t \mathbf{R}_n^{-l} \mathbf{H} + \mathbf{R}_x)^{-1} \mathbf{H}^t \mathbf{R}_n^{-l}\right] \mathbf{z} = \mathbf{B}\mathbf{z} \qquad (4)$$

The terms in equation 4 can be consolidated into a single reconstruction matrix $\mathbf{B}$. In order to estimate $\hat{\mathbf{x}}$ using a subset of the available measurements, the noise variance term $\mathbf{R}_n$ on all unused measurements in (4) is set to ∞ (Adler, 2004). This has the effect of introducing zeros into $\mathbf{R}_n^{-1}$ at positions on the diagonal corresponding to the unused measurements. $\mathbf{R}_x$ represents the spatial correlation between the finite element conductivities in the forward model; while $\mathbf{R}_x^{-1}$ is the regularization prior, modelled as a spatial high pass filter. Even though our results are based on the reconstruction algorithm of Adler and Guardo (1996), this approach does not depend on the details of the regularization framework, and can be used for any one step reconstruction algorithm. We introduce the notation $\mathbf{B}(e_i, e_j)$ for the reconstruction matrix designed not to use measurements made with electrodes e_i and e_j.

We elaborate this technique for the adjacent current injection pattern, but it is applicable to other EIT stimulation patterns, such as opposite and interleaved current drive patterns (Eyüboğlu, 1996). Two adjacent electrodes are used for current injection and the remaining electrodes are used to make voltage measurements as shown in Fig. 1. Overall, there are N×(N-3) measurements available when all electrodes give good data. However, when there is one erroneous electrode, the total number of measurements available is reduced to (N-3)×(N-4). Typically, with sixteen electrodes the remaining "good" data are sufficient to reconstruct a reasonable image (Adler, 2004).

Detection of erroneous electrodes

In order to detect erroneous electrodes, we rephrase the problem to instead detect sets of good (not erroneous) electrodes, from which the erroneous electrodes are excluded. As mentioned previously, a set of good electrodes produces internally consistent data. Such consistency can be verified by estimating the measured data at each electrode in the set, using only measurements on other electrodes, and then comparing the estimate to the actual data measured. Thus, our method analyses difference EIT data from a set of electrodes S, in order to detect the presence of a single erroneous electrode. Fig. 2 outlines the basic steps of the method.

We iterate over each electrode e_i in S, forming a set S' of all electrodes not including e_i. S' is then tested to calculate a parameter T_i which reflects the consistency of measurements among electrodes in S', and is the sum of estimation errors for all electrodes not including i. The estimation error for an electrode j is defined as:

$$E_j = \left\| \mathbf{z}_j - \hat{\mathbf{z}}_j \right\|_2^2 \tag{5}$$

Figure 4 shows a block diagram of steps for calculating E_j. $\mathbf{z}_j$ is the vector of normalized differential measurements made using e_j, and $\hat{\mathbf{z}}_j$ is the estimate of $\mathbf{z}_j$ based on all electrodes in S′ except e_j (Fig. 3), which is calculated by:

$$\hat{\mathbf{z}}_j = \mathbf{H}_j \hat{\mathbf{x}} \tag{6}$$

where $\mathbf{H}_j$ represents the rows of the sensitivity matrix $\mathbf{H}$ which correspond to measurements on e_j. $\hat{\mathbf{x}}$ is then calculated from (4), without data from electrodes e_i and e_j as

$$\hat{\mathbf{x}} = \mathbf{B}(e_i, e_j)\mathbf{z} \qquad (7)$$

It is necessary to calculate (7) without electrodes e_i and e_j because e_i is not part of S', and e_j is the electrode being estimated.

In order to efficiently compute $\mathbf{E}_j$ in S'', we define a selector matrix, $\mathbf{S}_j$, such that $\mathbf{z}_j = \mathbf{S}_j\mathbf{z}$ to isolate the data from electrode e_j. Thus, (5) becomes

$$\mathbf{E}_j = \left\| \mathbf{S}_j[\mathbf{z} - \hat{\mathbf{z}}] \right\|_2^2 \qquad (8)$$

Substituting $\hat{\mathbf{z}}$ with (6) and (7)

$$\mathbf{E}_j = \left\| \mathbf{S}_j[\mathbf{z} - \mathbf{HB}(e_i, e_j)\mathbf{z}] \right\|_2^2 \qquad (9)$$

which can be written

$$\mathbf{E}_j = \mathbf{z}^T(\mathbf{I} - \mathbf{B}(e_i, e_j)^T\mathbf{H}^T)\mathbf{S}_j^T\mathbf{S}_j(\mathbf{I} - \mathbf{HB}(e_i, e_j))\mathbf{z} \qquad (10)$$

in which the term $(\mathbf{I} - \mathbf{B}(e_i, e_j)^T\mathbf{H}^T)\mathbf{S}_j^T\mathbf{S}_j(\mathbf{I} - \mathbf{HB}(e_i, e_j))$ may be precomputed, since it does not depend on the data.

If all values of T_i are low, S′ contains all "good" electrodes, otherwise it contains at least one erroneous electrode. T_i values are tested against each other to detect if any are

significantly less than the others. We have developed a simple heuristic measure (*PER*) to measure this property. Initially, we define a parameter D

$$\mathbf{D}_i = \sum_{j=1}^{16} \left(T_i - T_j \right) \tag{11}$$

Data with no error will have comparable *T* values, small variation in **D**, and a ratio of maximum to minimum **D** close to one. We express this ratio in dB and call it prediction error ratio (*PER*):

$$PER = 20 \log \left[\frac{\max(\mathbf{D})}{\min(\mathbf{D})} \right] \tag{12}$$

A low *PER* indicates that the *T* values are close to one another and the data is consistent, while a high *PER* value indicates an erroneous electrode. *PER* is used to detect the presence of an erroneous electrode, and subsequently, *T* is used to identify it.

Data

EIT data were obtained from previous experiments (Adler *et al*, 1997). Mechanically ventilated mongrel dogs had sixteen ECG-style electrodes spaced evenly around the shaved thorax 10 cm above the base of the rib cage, and adjacent drive EIT measurements were acquired. Four animals, of nineteen, showed some level of electrode errors. Images were calculated corresponding to data measured at each inspiration. The gold standard for electrode error was based on human assessment. A graphic user interface was developed to evaluate test images by five experienced users, who were asked to classify each image as either: *no error*, *possible error*, or *definite error*. Identification of images with no error was consistent, but there were varying assessments of images considered to have possible error and definite error. We used the majority opinion to classify images.

Results

This method was implemented in Matlab; using a FEM mesh of 256 elements on an Athlon 1.8GHz computer, it requires 74 s to pre-compute the values in (10) and a further 3 s to calculate *PER* and *T* for each EIT difference data set.

Tests with simulated data: Fig. 5A shows EIT data classified as *no error*. The graph of *T* vs. electrode number (Fig. 5A) shows consistent values of *T* corresponding to a *PER* of -13dB, which indicates good electrodes. Fig 5B shows the reconstructed image of data from Fig. 5A with additive white Gaussian noise (SNR= 9dB) to the data of electrode 4. The resulting reconstructed image is poor with large artefacts. When the method is applied to these data, *T* values from all electrodes except electrode 4 are consistent (Fig. 5, bottom), which suggests that electrode 4 is erroneous.

Tests with experimental data: Three sets of representative EIT data of ventilated dogs were used: data with no error (Fig. 6A), a small error (Fig. 6B), and a larger error (Fig. 6C) (based on our experience of EIT errors). The reconstructed images and graphs of *T* vs. electrode number are shown. Data with errors (Fig. 6B and Fig. 6C) show higher overall values of T_i , compared to error free data (Fig. 6A). In Fig. 6C, the electrode with errors has significantly lower T_i ($p<0.05$). In the case of Fig. 6C, two adjacent electrodes are detected. We have noted that this is not uncommon result for this method with larger data errors. Based on our experience with this data set, we believe that the adjacent electrodes are both erroneous. Figure 7 shows *PER* as a function of SNR for a range of values (-50 dB to 50 dB). PER (± std dev) was calculated based on 100 simulations at

each SNR value. This method can reliably detect an erroneous electrode when the SNR is
below approximately 20dB. Such a level of SNR has an imperceptible visual impact on
the reconstructed image.

Discussion

This paper presents a method to automatically detect an erroneous electrode in EIT data. It is based on measuring the consistency of data amongst all electrodes to identify the ones producing inconsistent measurements. Results show that the method is able to correctly detect the presence and identify the location of erroneous electrodes in experimental and simulation data. The detection threshold is determined using the *PER* vs. SNR graph (Fig. 7). We recommend a threshold of PER = -22dB. In comparing the results obtained from the method to the user classification, both the method and the user classification generated a comparable percentage of *definite error* data, 28% and 25%. The method detected 57% of the images as *no error*, while the user classification provided 67%, probably due to some errors not being visible in the reconstructed image. After detection of an erroneous electrode it would be possible, in a real time measurement scenario, to identify and correct the underlying problem. If data collection is already complete, it would be possible to compensate for the erroneous electrode using a technique such as that of Adler (2004). Figure 8 shows an example of such compensation. The large number of erroneous electrodes was caused by the animal's poor skin condition.

This method was also evaluated using simulated data for an opposite drive pattern and shows similar results to those in Fig 5. Tests were carried out to evaluate the performance using different size finite element meshes, other than the 256 element mesh used for the results in this paper. A finer mesh grid (>256 elements) results in longer execution time with a slight increase in separation of *T* values for erroneous electrodes.

Even though this method was not developed to detect multiple electrode errors, the results (Fig. 6C) appear to show the ability to detect two adjacent erroneous electrodes. The T value decreases at an erroneous electrode position because the error contribution from that electrode is eliminated. In the case of multiple erroneous electrodes, part of the error contribution is removed even though contribution from other electrodes remains. Thus, the technique can detect multiple erroneous electrodes, although with reduced sensitivity. To test this result, a data set with no errors was selected and varying levels of white Gaussian noise added to two adjacent electrodes. Results show that the two adjacent electrodes have a significantly lower T value than the remaining electrodes. A better approach to detect two erroneous electrodes would be selecting two or more candidate electrodes in the set S, and calculating the respective $\mathbf{E}_j$ for all e_j in S'.

This method for detection erroneous electrodes could also be used for static EIT applications. Static EIT is more sensitive than difference EIT to measurement errors (Korjenevsky, 1995), and management of these errors is important for algorithm stability. Since an electrode error should be present whether measurements are interpreted as static or difference data, we propose that the method described here could be applied in static EIT by performing the test for errors on sets of EIT difference measurements, while the actual reconstruction is done statically.

Automatic detection of electrode errors in EIT has several possible applications. In offline processing, such a technique could identify and correct for such errors. More usefully, if implemented in EIT monitoring equipment, it would be possible to alert staff

who could then attend to the problem. However, for such online applications, the algorithm is not real-time (3s per data set with a pre-processing time of one minute), but would permit erroneous error detection as a separate process.

References

Adler A and Guardo R 1996 Electrical Impedance Tomography: Regularised imaging and Contrast Detection, *IEEE Trans. Medical Imag.* **15** 170-179

Adler A 2004 Accounting for erroneous electrode data in Electrical Impedance Tomography *Physiol. Meas.* **25** 227-238

Adler A, Amyot R, Guardo R, Bates J H T and Berthiaume Y 1997 Monitoring changes in lung air and liquid volumes with electrical impedance tomography *J. Appl. Physiol.* **83** 1762-1767

Al-Hatib F 1998 Patient-instrument connection errors in bioelectrical impedance measurement, *Physiol. Meas.*, **19** 285-296

Blott B H, Daniell G J and Meeson S 1998 Electrical impedance tomography with compensation for electrode positioning variations *Phys. Med. Biol.* **43** 1731-1739

Eyüboğlu B M 1996 An interleaved drive electrical impedance tomography image reconstruction algorithm *Physiol. Meas.* **17** A59–A71

Korjenevsky A. V., Kornienko V. N., Kul'tiasov M. Yu., Yu. S. Kul'tiasov, and Cherepenin 1997 Electrical Impedance Computerized Tomograph for Medical Applications *Instruments and Experimental Techniques* **40** 415-421

Lozano A, Rosell J and Pallás-Areny R 1995 Errors in prolonged electrical impedance measurements due to electrode repositioning and postural changes *Physiol. Meas.* **16** 121-130

Meeson S, Blott B, and Killingback A 1996 EIT data noise evaluation in the clinical environment *Physiol. Meas.* **17**(suppl.) A33-A38

Figure 1:

	01	12	23	34	45	56	67	70
01	X	X		*	*			X
12	X	X	X	*	*			
23		X	X	X	*			
34	*	*	X	X	X	*	*	*
45	*	*	*	X	X	X	*	*
56				*	X	X	X	
67				*	*	X	X	X
70	X			*	*		X	X

Caption:

Data available for an eight electrode EIT system using adjacent drive with one erroneous electrode. The vertical axis represents electrode pairs used for current injection and the horizontal axis those used for voltage measurement. ″**X**″ represents data not available from electrodes used for current injection. ″*″ represents data lost when electrode 4 is erroneous.

Figure 2:

Define set $S = \{\, e_i \mid i = 1....N\}$
For all e_i in S
        Define set, S', without electrode e_i: $S' = \{\, e_i : j = 1....N,\ j{\neq}i\}$
        For all e_j in S'
                Calculate image: $\hat{\mathbf{x}} = \mathbf{B}(e_i, e_j)\mathbf{z}$
                Estimate measurements on e_j: $\hat{\mathbf{z}}_j = \mathbf{H}_j\hat{\mathbf{x}}$
                Calculate: $\mathbf{E}_j = \left\| \mathbf{z}_j - \hat{\mathbf{z}}_j \right\|_2^2$
            Calculate: $T_i = \sum\limits_{j=1, j \neq i}^{N} E_j$
If T_i is significantly less than other values of T, **detect** e_i as erroneous electrode

Caption:

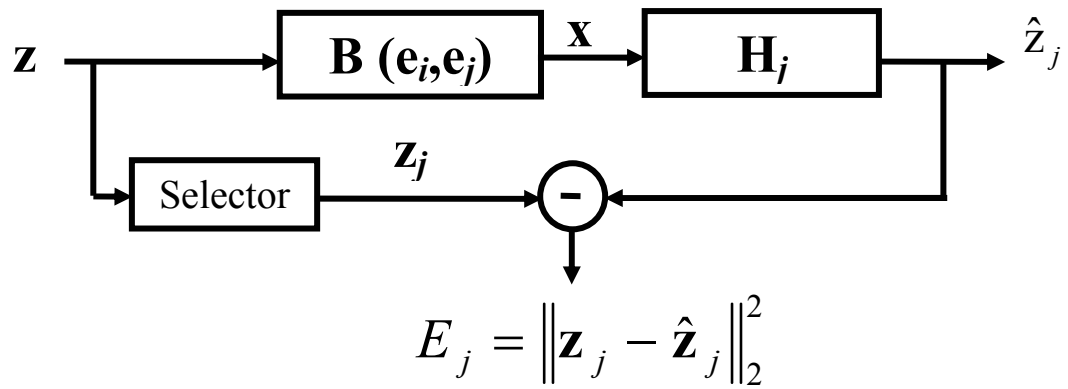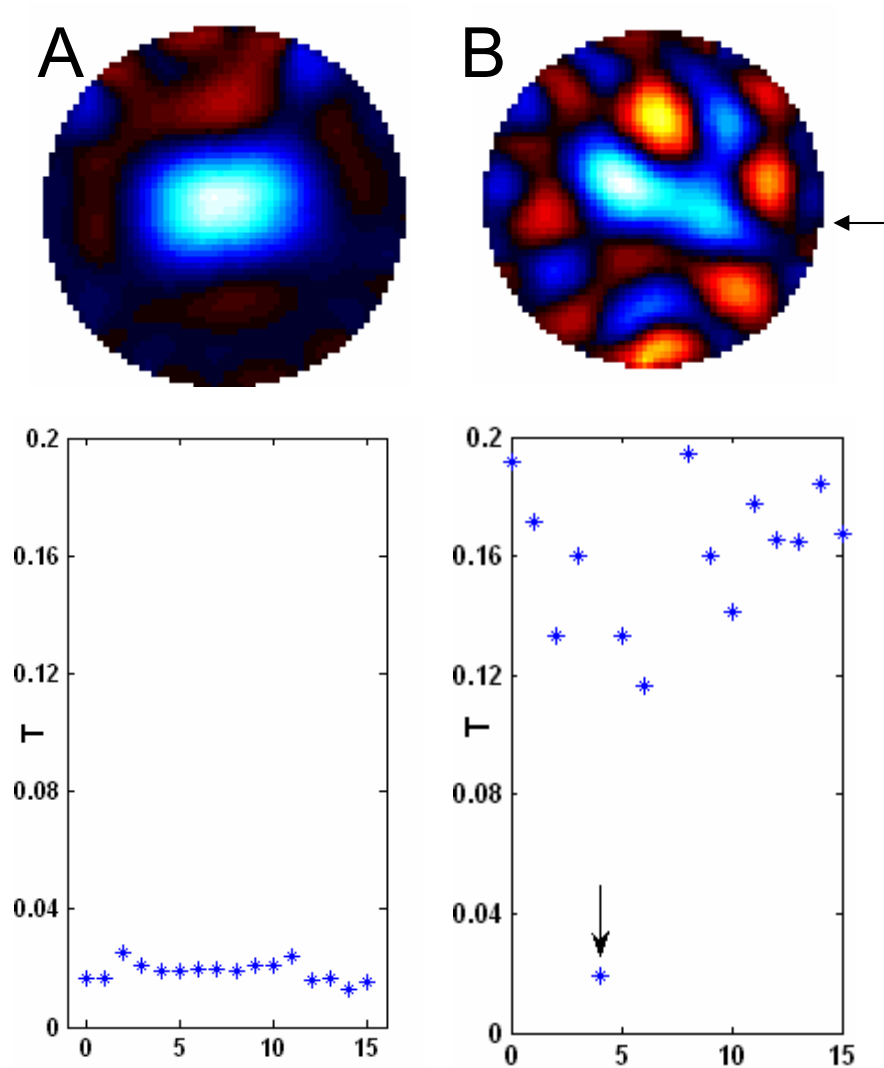Pseudo code for detection of an erroneous electrode.

Figure 3:
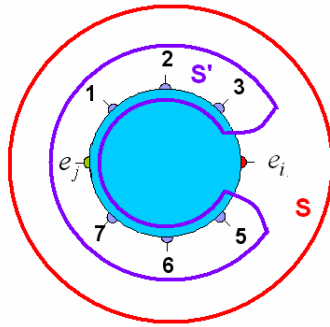
Caption:

Illustration of electrode sets *S* and *S'*. To test electrode 4, the estimation error $\mathbf{E}_j$ is calculated for each electrode in set *S'*.

Figure 4:

$$E_j = \left\| \mathbf{z}_j - \hat{\mathbf{z}}_j \right\|_2^2$$
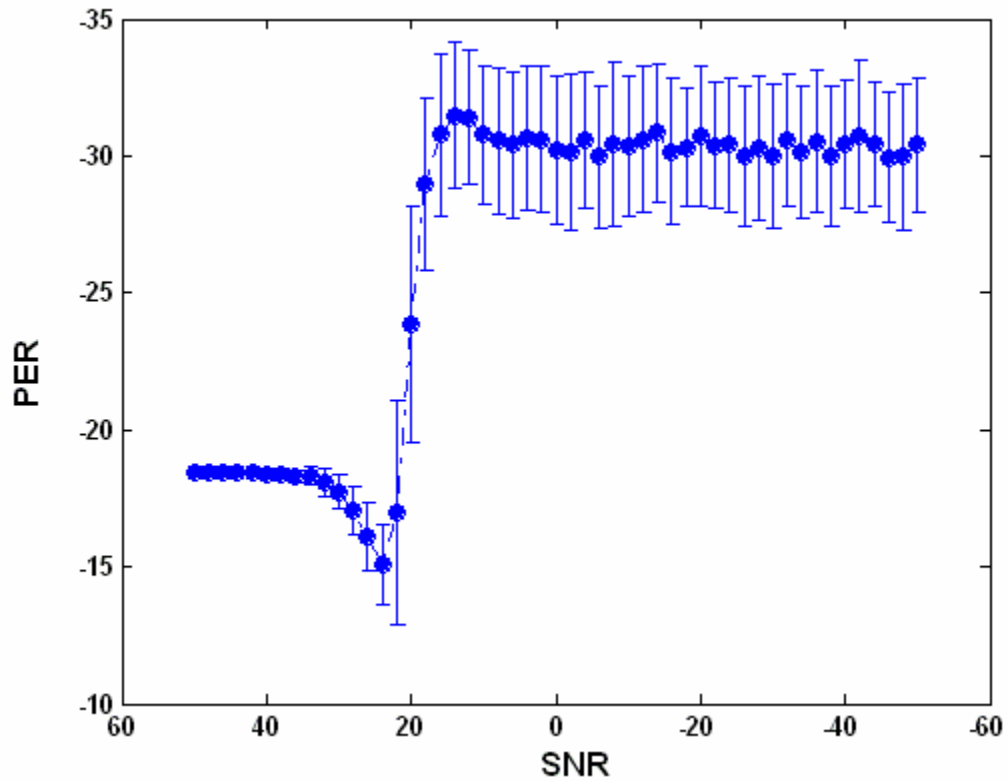
Caption:

Block diagram of calculation for estimation error $\mathbf{E}_j$

Figure 5:

Caption:

Upper row: images of tidal ventilation in a dog with and without simulated noise. Electrodes are numbered clockwise with electrode zero at the top centre. Images are individually normalized to the colourscale (arbitrary units) at right. *Bottom row*: parameter T for each electrode. (A) no erroneous electrode (B) simulated error (9dB SNR) on data from electrode 4. The arrow indicates the location of the erroneous electrode.

Figure 6:
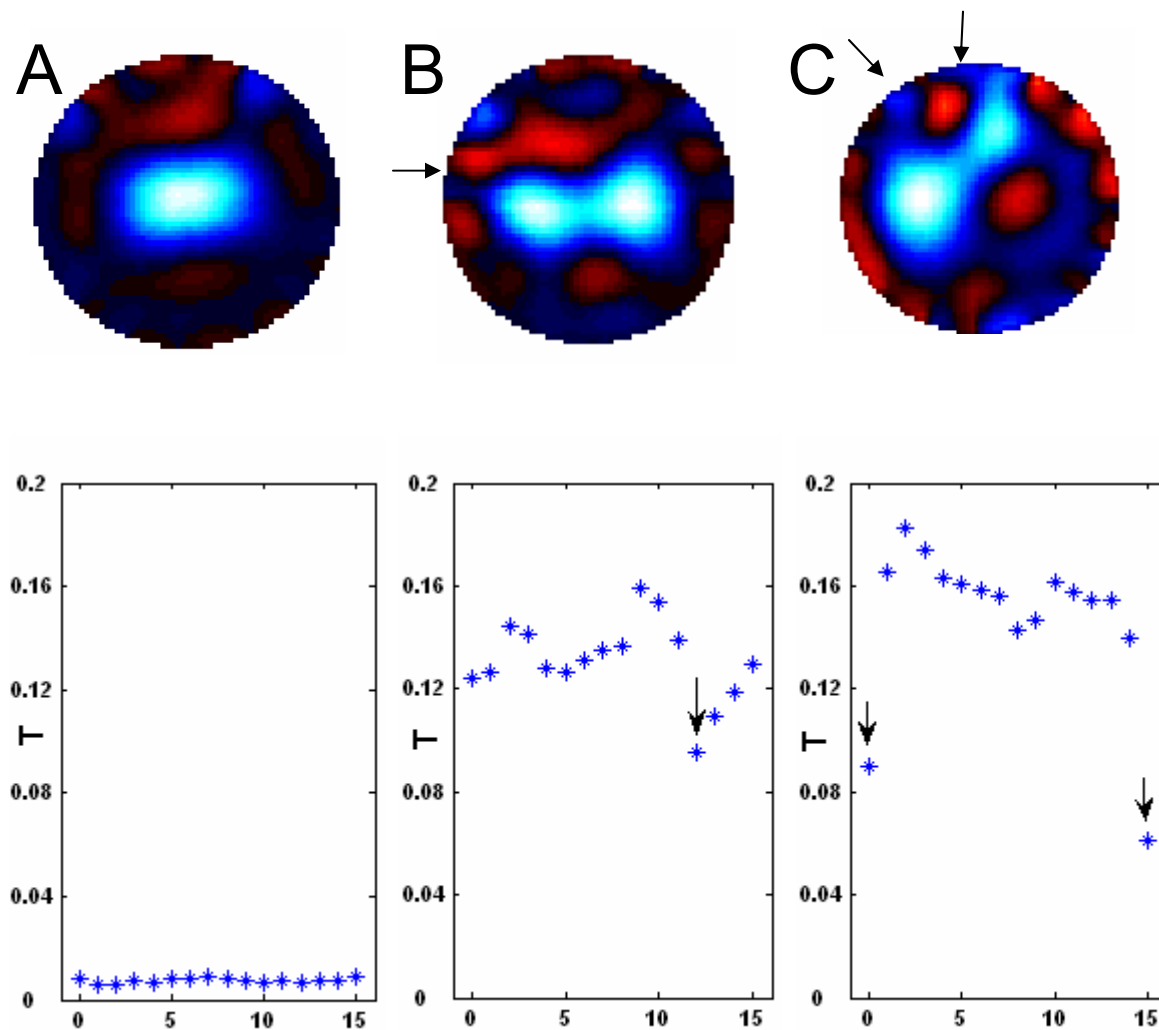
Caption:

Upper row: A, B and C: images of tidal ventilation in a dog. Electrodes are numbered clockwise with electrode zero at the top centre. Images are individually normalized to the colourscale (arbitrary units) at right. *Bottom row*: parameter *T* for each electrode (A) no erroneous electrode (B) data with erroneous electrode with small error signal. (C) data with erroneous electrode with typical error signal. Arrows show the location of the erroneous electrode(s).

Figure 7:

Caption:

PER vs. *SNR* using simulated white Gaussian noise on data from tidal ventilation in a dog (100 simulations per data point). For SNR greater than 20dB, *PER* shows a significant jump. We use a threshold of detection of *PER* = -22 dB.

Figure 8:
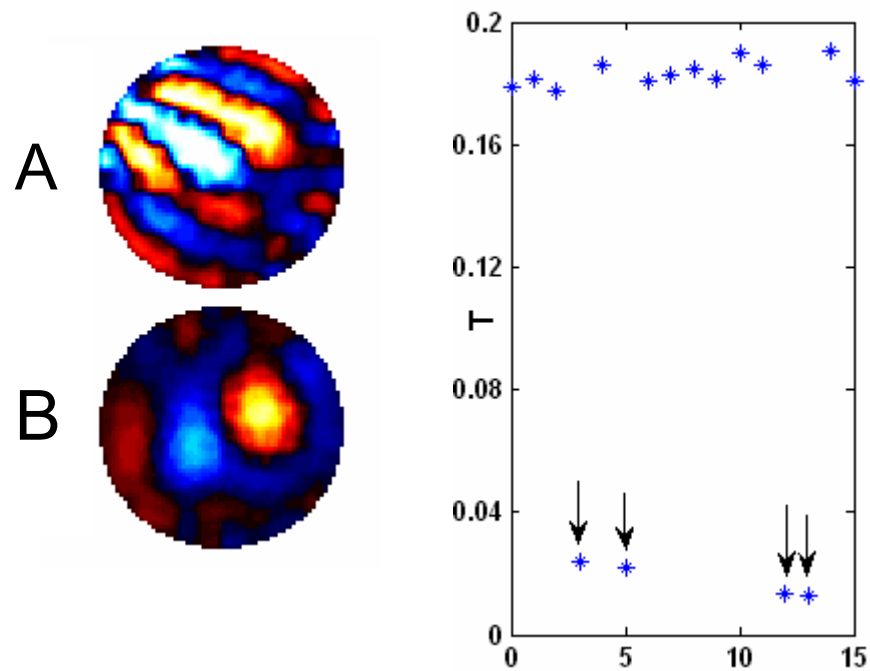
Caption:

Left (A): difference image of 700ml inspiration and 100ml right lung fluid installation in a dog. Electrodes are numbered clockwise with electrode zero at the top centre. Both images normalized to same colourscale. (B): Image of data from (A) using the method of Adler (2004) to compensate for the erroneous electrodes identified below. *Right*: *T* for each electrode in (A). Based on these data, electrodes 3, 5, 12, 13 were identified as erroneous.